Eco-Evolutionary Metapopulation Dynamics and the Spatial Scale of Adaptation

Ilkka Hanski,* Tommi Mononen, and Otso Ovaskainen

Department of Biosciences, University of Helsinki, P.O. Box 65, FI-00014 University of Helsinki, Finland

Submitted September 17, 2010; Accepted October 4, 2010; Electronically published November 19, 2010

Online enhancements: appendixes.

ABSTRACT: We construct a model that combines extinction-colonization dynamics with the dynamics of local adaptation in a network of habitat patches of dissimilar qualities. We derive a deterministic approximation for the stochastic model that allows the calculation of patch-specific incidences of occupancy and levels of adaptation at steady state. Depending on (i) the strength of local selection, (ii) the amount of genetic variance, (iii) the demographic cost of maladaptation, (iv) the spatial scale of gene flow, and (v) the amount of habitat heterogeneity, the model predicts adaptation at different spatial scales. Local adaptation is predicted when there is much genetic variance and strong selection, while network-level adaptation occurs when the demographic cost of maladaptation is low. For little genetic variance and high cost of maladaptation, the model predicts network-level habitat specialization in species with long-range migration but an intermediate scale of adaptation (mosaic specialization) in species with short-range migration. In fragmented landscapes, the evolutionary dynamics of adaptation may both decrease and enhance metapopulation viability in comparison with no evolution. The model can be applied to real patch networks with given sizes, qualities, and spatial positions of habitat patches.

Keywords: eco-evolutionary dynamics, local adaptation, network adaptation, habitat specialization, cost of maladaptation, habitat fragmentation.

Introduction

Adaptive divergence of populations in fitness-related traits is generally negatively correlated with the magnitude of gene flow (Gandon et al. 1996; Hendry et al. 2001; Bolnick et al. 2008; recent analyses include Morgan et al. 2005; Räsänen and Hendry 2008; Nosil 2009; North et al. 2011). Negative association may be due to gene flow hindering local adaptation and hence adaptive divergence, but causality may also work the other way, with gene flow being hindered by populations having become adapted to dissimilar environments. The former is usually assumed (Räsänen and Hendry 2008) and supported by field experiments (Riechert 1993; Nosil 2009), but there are also putative examples of the latter (Kuussaari et al. 2000; Hanski and Singer 2001; Edelaar et al. 2008). In some situations, gene flow may facilitate rather than prevent local adaptation by increasing additive genetic variance in focal populations. This may happen in coevolutionary dynamics between hosts and pathogens (Gandon et al. 1996; Gandon and Michalakis 2002; Thompson et al. 2002; Morgan et al. 2005), in sink populations (Holt and Gomulkiewicz 1997; Gomulkiewicz et al. 1999), and in situations where migration is biased toward local populations living under similar environmental conditions (Byars et al. 2009). Genetic drift in small populations may swamp selection, which may explain apparent lack of local adaptation in small plant populations (Leimu and Fischer 2008).

The conventional view of local adaptation assumes stable local populations in which the phenotypic distribution approaches an equilibrium. In the case of two or more coevolving species and under changing environmental conditions, the optimal phenotype is, however, a moving target, and the process of local adaptation does not come to a halt. The concept of the geographic mosaic of coevolution (Thompson 2005) is concerned with such complex dynamics. In metapopulations consisting of extinction-prone local populations inhabiting a heterogeneous environment, local adaptation can be expected to continue forever because new populations are often established by individuals that are initially poorly adapted to the local environmental conditions. Furthermore, in metapopulations, the spatial scale of adaptation may be the scale of local populations, but adaptation may also occur at larger spatial scales as species may become adapted to the environmental conditions in a network of habitat patches rather than in single patches. This is especially likely to happen in classic metapopulations with fast population turnover.

Studies on the *Linum marginale–Melampsora lini* plant-pathogen interaction have revealed a hierarchical spatial

* Corresponding author; e-mail: ilkka.hanski@helsinki.fi.

Am. Nat. 2011. Vol. 177, pp. 29–43. 0003-0147/2011/17701-52480$15.00.
DOI: 10.1086/657625

structure of adaptation involving adaptation within local populations but also at the regional (metapopulation) scale (Thrall et al. 2002). In another plant pathogen study, Laine (2005) demonstrated that the fungus *Podosphaera plantaginis* becomes adapted to host resistance at the level of networks of small local populations rather than at the level of the local populations themselves. Toju's (2008) study of spatial variation in the coadaptation of the mouthpart length of the weevil *Curculio camelliae* and the pedicarp thickness of its host plant *Camellia japonica* is another example in which adaptation is thought to occur at both the local and regional scales. A series of studies by Nosil and collaborators (Nosil 2009 and references therein) on the walking stick insect *Timema cristinae*, though primarily concerned with pairs of populations, nonetheless strongly suggests the possibility of network-level adaptation. In other words, the degree of adaptation in a particular population depends on the connectivity of the population to other populations with dissimilar adaptations due to dissimilar environmental conditions.

The Glanville fritillary butterfly (*Melitaea cinxia*) in the Åland Islands in Finland, where it has a classic metapopulation structure in a network of ~4,000 dry meadows (Hanski 1999; Nieminen et al. 2004), offers another metapopulation-scale example. There are two host plant species, *Plantago lanceolata* and *Veronica spicata*, with spatial variation in their relative abundances among the meadows within regional networks, as well as at the scale of the entire Åland Islands (Kuussaari et al. 2000). The female host plant preference has high heritability (Singer and Hanski 2004; Klemme and Hanski 2009), a necessary condition for fast adaptation. In this system, spatial variation in host plant use reflects adaptation at the scale of regional networks rather than at the scale of local populations (Heino and Hanski 2001; Hanski and Heino 2003), which is not unexpected because local populations are often very small and have short lifetimes (Hanski 1999; Nieminen et al. 2004).

Stimulated by these studies, we construct and analyze a metapopulation model that combines stochastic extinction-colonization dynamics and the dynamics of local adaptation. The coupling between the two is due to several factors. First, immigrants have phenotypes that reflect the populations from which they originate. Second, the rate of establishment of new populations may depend on the match between the phenotype of the immigrants and the local environmental conditions. Finally, the rate of population extinction may depend on the degree of maladaptation of local populations. In this model, spatial demographic dynamics affect local adaptation and vice versa, and the coupled dynamics may lead to adaptation at spatial scales ranging from individual local populations to the entire network.

In the next section, we construct a stochastic eco-evolutionary model combining extinction-colonization dynamics and the dynamics of local adaptation, and we derive a deterministic approximation of the stationary state of the stochastic model to facilitate model analysis. We analyze how the predicted spatial scale of adaptation, whether local or regional, and the degree of habitat specialization depend on the strength of selection, the cost of local maladaptation, and the spatial range of migration and hence of gene flow. For a range of parameter values, the model exhibits alternative locally stable states at the metapopulation scale, represented by habitat specialists adapted to different habitat types and by habitat generalists that are not well adapted to any type. In large networks, different kinds of habitat specialists may occur in different parts of the network, yielding a mosaic pattern of specialization. We also examine how the evolutionary dynamics of local adaptation affect the demographic viability of metapopulations in increasingly fragmented landscapes, and we find that evolution may both enhance and reduce metapopulation viability. The model is spatially realistic (Hanski 2001) in the sense that it assumes a finite patch network with given patch areas, qualities, and connectivities, making it possible to fit the model to empirical data and to predict spatial patterns in adaptation across real patch networks.

Models

We start by constructing a continuous-time stochastic patch occupancy model (Moilanen 2004; Ovaskainen and Hanski 2004) for a metapopulation inhabiting a finite network of habitat patches ("Stochastic Patch Occupancy Model"). The rate of change in the mean phenotype in each local population is described with a deterministic model from colonization until extinction, with the mean phenotype at colonization giving the initial value. We next derive expressions for the extinction and colonization rates that depend on the spatial structure of the landscape: patch areas, qualities, and spatial connectivities ("Extinction and Colonization Rates"). These expressions include eco-evolutionary feedbacks, such as maladaptation increasing the rate of local extinction. Finally, in "Deterministic Approximation" we derive a deterministic approximation for the stationary state of the full stochastic model; the approximation offers insight into the model and facilitates its analysis. Technical details are given in appendix B in the online edition of the *American Naturalist.*

Two important simplifying assumptions of the stochastic model and its approximation are constant additive genetic variance and lack of genetic drift in local populations. These assumptions are potentially restrictive, but we show in appendix A in the online edition of the *American Nat-*

uralist that the model gives a good approximation of the stationary state of an individual-based model in which genetic variance and drift are modeled mechanistically.

Stochastic Patch Occupancy Model

We model the presence or absence of a species in a finite network of habitat patches. The demographic model is a Markov process specified by the rates of colonization of the currently empty patches and the rates of extinction of local populations in the currently occupied patches. We denote the occupancy state (1 or 0) of patch i by $O_i(t)$ and the respective mean phenotype, defined for the occupied patches only, by $Z_i(t)$. We assume that the additive genetic and environmental variances σ_G^2 and σ_E^2 are constants over time and equal for all local populations and that the total phenotypic variance is given by the sum $\sigma_P^2 = \sigma_G^2 + \sigma_E^2$. The colonization rate of patch i at time t is given by

$$C_i(t) = \sum_{j \neq i} m_{ij} O_j(t), \tag{1}$$

where m_{ij} is the contribution of patch j with the mean phenotype $Z_j(t)$ to the colonization rate of patch i (we write here and below m_{ij} instead of $m_{ij}(Z_j(t))$ to simplify the notation). At colonization, the newly established population acquires the average phenotype of the colonizers. We assume the migrant pool model of colonization (Slatkin 1977), in which case the mean phenotype of population i at colonization is given by

$$Z_i^C(t) = \frac{\sum_{j \neq i} m_{ij} O_j(t) Z_j(t)}{C_i(t)}. \tag{2}$$

In other words, the mean phenotype of a newly established population is the weighted average of the mean phenotypes in the source populations, the weights being the contributions m_{ij} of the source populations to the colonization of patch i.

Following colonization, the mean phenotype is affected by selection and gene flow. The optimal phenotype, denoted by θ_i, depends on the environmental quality of patch i but remains constant in time. The rate of change in $Z_i(t)$ is given by

$$\frac{dZ_i(t)}{dt} = \gamma \sigma_G^2 (\theta_i - Z_i(t)) + \frac{\rho}{A_i} \sum_{j \neq i} m_{ij} (Z_j(t) - Z_i(t)) O_j(t), \tag{3}$$

where γ is the strength of stabilizing selection (Ronce and Kirkpatrick 2001). The second term is due to gene flow and shows that the mean phenotype in patch i can be both increased and decreased by gene flow, depending on the mean phenotypes in the source populations. The model assumes normally distributed phenotypic values. Deviations from the Gaussian distribution tend to reduce the effect of gene flow on local adaptation (Yeaman and Guillaume 2009).

The term for gene flow in equation (3) may be rewritten as $(\rho C_i(t)/A_i)(Z_i^C(t) - Z_i(t))$, showing that gene flow is proportional (parameter ρ) to colonization rate (eq. [1]) and is hence influenced by all the parameters that determine the contribution of population j to colonization of patch i (these parameters will be specified in the next subsection; eq. [7]). Additionally, gene flow is assumed to be inversely proportional to patch area A_i, which is used here as a surrogate of (the expected) population size when patch i is occupied. We make this assumption because the rate of change in the mean phenotype depends on gene flow, that is, absolute numbers of immigrants that reproduce in proportion to the size of the resident population. By changing the value of ρ, we may adjust the relative strength of gene flow in relation to founder events. The extinction rate $E_i(Z_i(t))$ of population i may depend on the mean phenotype as described in the next subsection.

Extinction and Colonization Rates

We next specify how maladaptation and small expected population size increase the extinction rate and how the spatial configuration of the patch network affects the colonization rate (for comparable metapopulation models, see Hanski and Ovaskainen 2003; Ovaskainen and Hanski 2004). The structure of the finite patch network is specified by the areas A_i, the habitat qualities Q_i, and the spatial positions (coordinates x_i and y_i) of the patches.

Though we do not model changes in the sizes of local populations but only the changing pattern of patch occupancy, we derive below a semimechanistic expression for the growth rate of local populations, used to couple demographic dynamics with local adaptation. In the discrete-time ceiling model of population growth (Lande 1993; Foley 1994), population size at time $t + 1$ is given by

$$N_{t+1} = \min [R_t N_t, K], \tag{4}$$

where K is the population ceiling. The population becomes extinct if $N_{t+1} < 1$. The finite growth rate R_t is lognormally distributed with mean $\bar{r}$ (mean of $\ln R$) and variance v. Using the diffusion approximation, it can be shown that the expected time to population extinction starting at K is given by (Lande 1993; Foley 1994)

$$T = \frac{K^s}{s\bar{r}}\left[1 - \frac{1 + sk}{\exp(sk)}\right], \tag{5}$$

where $s = 2\bar{r}/v$ and $k = \ln K$. If the transient from the carrying capacity to the quasi-stationary state is ignored, the time until extinction is exponentially distributed (Ovaskainen and Meerson 2010), and we can convert the mean time to extinction to extinction rate (probability of extinction per unit time) as $E = 1/T$. The risk of population extinction is thus inversely related to population ceiling (carrying capacity), which is commonly observed (Diamond 1984; Schoener and Spiller 1987; Hanski 1999). Further, extinction risk increases with decreasing value of s, which reflects the strength of environmental stochasticity (Lande 1993; Foley 1994; Hanski 1998).

We assume that the variance v is the same in all populations but that the population ceiling K_i in patch i is proportional to patch area A_i. We further assume that the value of $\bar{r}_i$ in population i with mean phenotype $Z_i(t)$ is given by

$$\bar{r}_i(t) = r_0 - \frac{\gamma}{2}\sigma_P^2 - \frac{\gamma}{2}(\theta_i - Z_i(t))^2. \tag{6}$$

Here r_0 is the mean growth rate in a hypothetical population in which all individuals are perfectly adapted to the local habitat. The second term represents the evolutionary load due to phenotypic variance σ_P^2 and the third term the cost of stabilizing selection (Lande and Shannon 1996; Ronce and Kirkpatrick 2001). For short, we define $r_1 = r_0 - (\gamma/2)\sigma_P^2$.

In summary, in this model, the extinction rate of a local population is increased by several factors: first, by decreasing patch area, which is used as a surrogate of the expected population size when the patch is occupied; second, by decreasing intrinsic rate of population increase and by increasing variance, the latter reflecting the strength of environmental stochasticity; third, by increasing phenotypic variance; and, finally, by the demographic cost of maladaptation, which increases with increasing strength of selection and increasing mismatch between the current mean phenotype and the optimal phenotype.

Turning to the colonization rate, we assume that the contribution of patch j to the colonization rate of patch i depends on its carrying capacity K_j (used as a proxy of local population size) and the growth rate $\bar{r}_j$, on the area of the target patch i and on the distance d_{ij} between patches i and j:

$$m_{ij} = cK_j e^{\bar{r}_j} e^{-\beta|\theta_i - Z_j|} A_i \frac{\alpha^2}{2\pi} e^{-\alpha d_{ij}}, \tag{7}$$

where c is a colonization rate parameter, α is the parameter of the exponential dispersal kernel, and the factor $\alpha^2/2\pi$ ensures that the kernel integrates to 1 over the two-dimensional space (Ovaskainen and Hanski 2004). Equation (7) assumes that large local populations send out more migrants than do small ones, that populations with higher growth rate send out more migrants, that larger patches receive more migrants than do small ones (being larger targets for the immigrants), and that migration distances are limited. The term $e^{-\beta|\theta_i - Z_j|}$ models yet another possible coupling between demographic and evolutionary dynamics: the rate of immigration to patch i, and hence the corresponding colonization rate, may depend on the match between the phenotype of the immigrant and the quality of the target patch. Such immigrant selection may influence the rate of colonization, of which a clear-cut example has been documented for the Glanville fritillary butterfly in relation to female oviposition host plant preference (called the colonization effect by Hanski and Singer [2001]) and other examples are discussed by Edelaar et al. (2008). Parameter β models the strength of immigrant selection (no such selection if $\beta = 0$). Finally, note that though we describe m_{ij} as the contribution of population j to the colonization of patch i, this same term also influences gene flow (eq. [3]) whenever gene flow is included in the model ($\rho > 0$).

Deterministic Approximation

In the stationary state of the stochastic model, the probability of patch i being occupied, defined as $p_i = E[O_i(t)]$, is independent of time. The mean phenotype in a patch depends on the age of the population, as with time the mean phenotype evolves toward the patch-specific optimal phenotype. We denote by $z_i(\tau)$ the expected mean phenotype in patch i, conditional on the patch being occupied, where τ is population age (time since the last colonization event). The balance between local adaptation and maladaptation due to poorly adapted colonizers depends on population lifetime. Letting $\omega_i(\tau)$ denote the probability that the population in patch i survives at least until age τ and $e_i(\tau)$ the expected extinction rate of a population of age τ, we have

$$\frac{d\omega_i(\tau)}{d\tau} = -e_i(\tau)\omega_i(\tau),$$

with $\omega_i(0) = 1$. The distribution of population lifetimes can be computed from this equation (app. B). Throughout this article, we use an asterisk to denote the expected values of variables, such as the mean phenotype z, computed over the distribution of population lifetimes. In simulations of the stochastic model, this expectation can be computed

Table 1: Model parameters and their default values

Parameter	Value
Patch network	100 patches within a 10-by-10 square area
A_i	Area of patch i; log-transformed areas normally distributed with the default mean of 2.0 and variance of 0.5
$\delta = \lvert\theta^1 - \theta^2\rvert$	Difference in optimal phenotypes; default value 0.8
f^1	Frequency of patch type 1; default value 0.5
Local growth and colonization:	
$K_i = A_i \propto N_i$	Population ceiling = patch area; proportional to expected population size conditional on the patch being occupied
r_1	Growth rate of the optimal mean phenotype; default value 1
v	Variance of the growth rate; default value 1
c	Colonization rate
α	Inverse of range of migration
ρ	Proportionality between colonization rate and gene flow
β	Parameter measuring the strength of immigrant selection, that is, the effect of migrant phenotype on colonization
Local adaptation:	
γ	Strength of selection
σ_G^2	Amount of additive genetic variance

Note: In the calculation of the equilibrium incidences of patch occupancy and the mean phenotypes (eqq. [8], [9]), the default initial values were 0.5 and 0.5, respectively, for all i.

by sampling populations at random times during the periods when the respective patches are occupied.

As the stochastic model is nonlinear, the expectations cannot be solved exactly. In appendix B, we derive a deterministic approximation by ignoring spatiotemporal correlations in both patch occupancy and phenotypic values and making some other simplifying assumptions. In this case, the expectations p_i^* and z_i^* can be solved approximately as the fixed points of the equations

$$p_i^* = \frac{\sum_{j\neq i} m_{ij}^* p_j^*}{e_i^* + \sum_{j\neq i} m_{ij}^* p_j^*}, \tag{8}$$

$$z_i^* = \frac{\gamma\sigma_G^2\theta_i + [e_i^* + (\rho/A_i)\sum_{j\neq i} m_{ij}^* p_j^*] z_i^{C^*}}{\gamma\sigma_G^2 + e_i^* + (\rho/A_i)\sum_{j\neq i} m_{ij}^* p_j^*}, \tag{9}$$

where $z_i^{C^*} = \sum_{j\neq i} m_{ij}^* z_j^* p_j^* / \sum_{j\neq i} m_{ij}^* p_j^*$, $e_i^* = \mathrm{E}_i(z_i^*)$, and $m_{ij}^* = m_{ij}(z_j^*)$. We show in appendix C in the online edition of the *American Naturalist* that in most cases the equilibrium calculated by iterating these equations agrees closely with the quasi-stationary state of the stochastic model. Equations (8) and (9) offer insight into the effects of selection, founder events, and gene flow on the values of the mean phenotype in particular populations. A further advantage of these equations is the facility with which results can be calculated for ranges of parameter values and for different landscapes via fast numerical iteration. Finally, one may use the approximation to fit the model to empirical data, which would be more difficult if using the full stochastic model.

Results

Adaptations at Local and Network Levels

We calculated numerical results for a network of 100 patches with random spatial locations within a 10-by-10 square area (table 1). Patch areas are lognormally distributed if not stated otherwise. The patches are of two types, with optimal phenotypes θ^1 and θ^2. We denote by δ the difference $\lvert\theta^1 - \theta^2\rvert$ and by f^1 the frequency of type 1 patches, which are randomized among all the patches. The default values for r_1, the growth rate of local populations that corresponds to the optimal mean phenotype, and v, the variance of the growth rate, are set to 1 (table 1). The latter value is consistent with empirical estimates presented by Foley (1997), though there is much variation between species and environments. Our analysis below is focused on the remaining four parameters: c, the colonization rate parameter; α, the spatial scale of migration; γ, the strength of selection; and σ_G^2, the amount of genetic variance. In this subsection, we assume no gene flow to existing populations ($\rho = 0$) and no immigrant selection ($\beta = 0$). The consequences of gene flow and immigrant selection will be examined in the next subsection.

Let us first consider a species with long-range migration (small α), for which the value of $z_i^{C^*}$ is roughly the same in all habitat patches. Equation (9) shows that populations tend to be locally adapted ($z_i^* \approx \theta_i$) when selection is strong and there is much additive genetic variance and when the lifetime of local populations is long (large T_i). Note, however, that in heterogeneous patch networks there may be

much variation in the values of T_i and p_i^*, and hence, the degree of local adaptation also varies among the habitat patches. Figure 1*A* gives an example.

If the product $\gamma\sigma_G^2 T_i$ is small, there is more limited local adaptation. Now the type of adaptation depends on the demographic cost of maladaptation, which is set by the product $\gamma\delta^2$. When $\gamma\delta^2$ is small, maladaptation does not reduce population growth rate much and the species becomes adapted at the network level, with little spatial variation in the z_i^* values regardless of the local optimal phenotype θ_i. In this case, the average value of z_i^* across the network roughly matches f^1, the frequency of habitat type 1 in the network (fig. 2*A*). We call this situation network adaptation as opposed to local adaptation (table 2). Notice that in this case the species is a habitat generalist, not well adapted to either of the two habitat types.

In contrast, when $\gamma\delta^2$ is large, the species tends to specialize on the more common habitat type in the network (fig. 2*B*). The reason for such habitat specialization (table 2) is the high cost of maladaptation, which may be illustrated by calculating the metapopulation capacity of the patch network for constant values of z (same in all populations). The metapopulation capacity is a measure of patch network size that takes into account both the pooled area of habitat and the effect of fragmentation on metapopulation size and viability (Hanski and Ovaskainen 2000). The following formula gives a good approximation of metapopulation capacity (Ovaskainen and Hanski 2002):

$$\frac{\sum (C_i^* T_i^*)^2}{\sum C_i^* T_i^*}.$$

Figure 3 gives three examples for low, intermediate, and high cost of maladaptation ($\gamma\delta^2$). When $\gamma\delta^2$ is small, the size of the network as measured by metapopulation capacity is largest for species with intermediate constant z, whereas when $\gamma\delta^2$ is large, the network is largest for species with very small or very large z values (fig. 3). Therefore, the same network appears very different for different species with different constant mean phenotypes. For clarity, we note that the metapopulation capacity measures only the demographic consequences of specialization, while its value is generally not maximized by evolution.

Qualitatively similar results about adaptation are obtained for short-range migration (large α), with one important exception. For parameter values that yield habitat specialization for small α, a mosaic pattern of subnetwork specialization may emerge for large α (fig. 4*A*). In this case, the degree of local adaptation is less clearly related to T_i and p_i^* (fig. 1*B*) than in the case of long-range migration. Similarly, if we consider the relationship between the z_i^* values and the proportion of different habitat types in the landscape, the pattern is more blurred (fig. 2*C*, 2*D*) than in species with long-range migration, due to the tendency toward spatial correlation in the mean phenotype. We call this pattern mosaic specialization (table 2).

Figure 5 (*top row*) illustrates the influence of three model parameters, γ, σ_G^2, and α, on the pattern of adaptation predicted by the model. The classification of the different types of adaptation is based on the diagnostic variables shown in figure C5 in appendix C. It should be noted that for most parameter combinations, the model predicts patterns that are intermediate between the named types, and hence, the classification in figure 5 must be

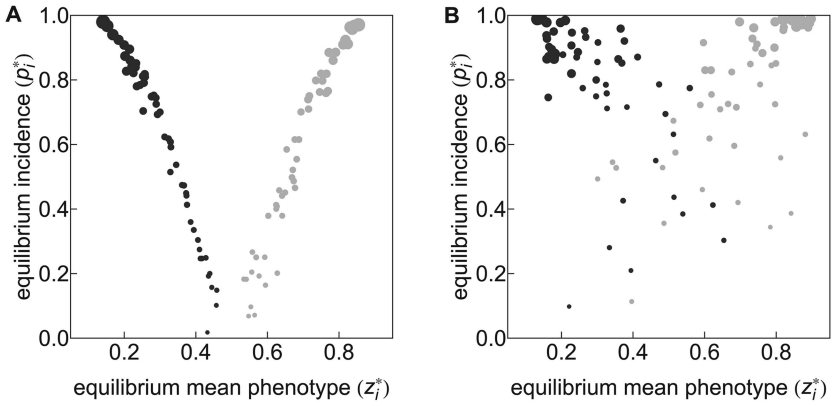

Figure 1: Incidence of patch occupancy at equilibrium (p_i^*) in relation to the respective mean phenotype (z_i^*) in species with large values of $\gamma\sigma_G^2 T_i$. *A*, Long-range migration ($\alpha = 0.2$); *B*, short-range migration ($\alpha = 2.0$). The other parameter values are $c = 0.002$, $\gamma = 1.5$, and $\sigma_G^2 = 0.023$. The patch network has the default structure and parameter values (table 1). Black and gray dots indicate patches with optimal phenotypes θ of 0.1 and 0.9, respectively.

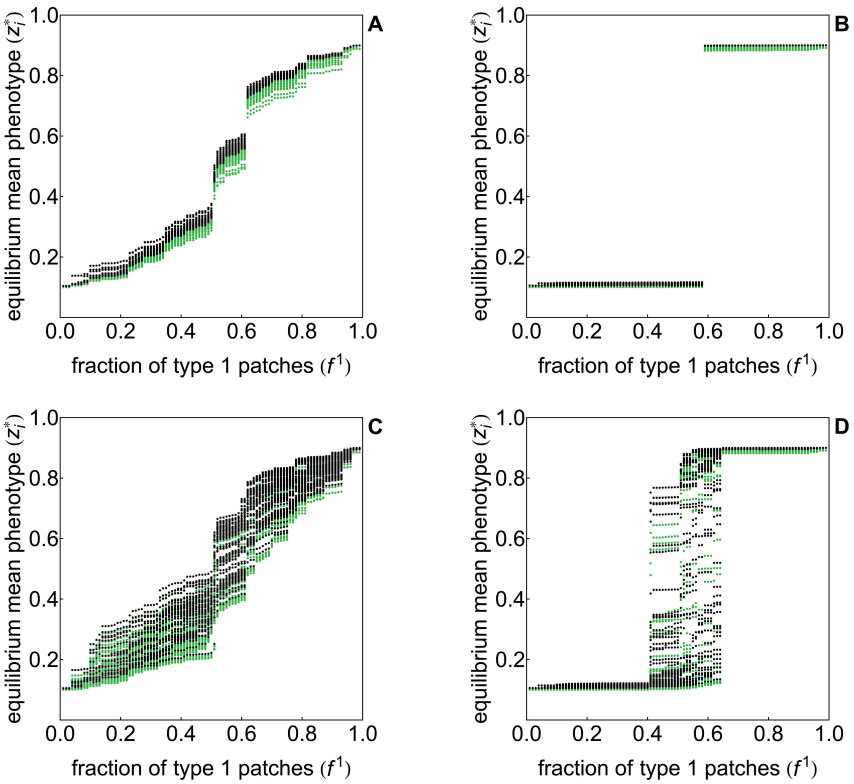

Figure 2: Distribution of equilibrium mean phenotypes (z_i^*) in relation to the frequency of type 1 patches (f^1) in the network. *A*, Example of network adaptation. Parameter values are $c = 0.002$, $\sigma_G^2 = 0.001$, $\gamma = 1$, and $\alpha = 0.2$. *B*, Example of habitat specialization. Parameter values are $c = 0.002$, $\sigma_G^2 = 0.001$, $\gamma = 5$, and $\alpha = 0.2$. *C*, *D*, As *A* and *B* but for short-range migration ($\alpha = 2.0$). The network has the default structure and parameter values (table 1). Black and green dots indicate patches with optimal phenotypes θ of 0.1 and 0.9, respectively.

interpreted accordingly. For instance, the pattern in figure 4 shows a clear spatially correlated pattern, yet by the criteria used in appendix C, it becomes classified as network adaptation.

It is apparent from figure 5 that regardless of the values of the other parameters, much genetic variance leads to local adaptation, while the more complex patterns occur when there is limited genetic variance. In the latter case, low cost of maladaptation (small γ) leads to network adaptation, while high cost of maladaptation (large γ) leads to either habitat specialization, in the case of long-range migration (small α), or mosaic specialization, in the case of short-range migration (large α). The colonization rate parameter c has a great influence on the incidences of patch occupancy but no major effect on the pattern of adaptation, though this will change when we include gene flow in the model. Decreasing the value of r_1 and increasing the value of v from default values (table 1) both increase the domains of habitat and mosaic specializations because such changes increase the cost of maladaptation.

Gene Flow and Immigrant Selection

In this subsection, we add gene flow to existing populations by setting $\rho > 0$. It is apparent from equation (9) that a general effect of gene flow is to reduce the influence of local selection on the z_i^* values and to reduce the part of the parameter space that is characterized by local adaptation (fig. 5, *middle row*). With long-range migration, the z_i^* values converge to a common value (z_i^{C*}) with increasing gene flow. With short-range migration, the model with moderate gene flow (fig. 4*C*) predicts mosaic specialization similar to that of the model without gene flow (fig. 4*A*), though spatial variation in the z_i^* values becomes somewhat reduced in the presence of gene flow. With more extensive gene flow, mosaic specialization is largely eliminated, and the model predicts either habitat specialization or network adaptation (fig. 5).

In the presence of gene flow to existing populations, the rate of migration (c) and hence the rate of gene flow affect the type of adaptation in patch networks with large dif-

Table 2: Four patterns of adaptation predicted by the model as a function of three combinations of parameters with an approximate description in words

Type of adaptation	Description	ΓT strength of local selection	Δ cost of maladaptation	$1/\alpha$ range of migration
Local adaptation	$z_i^* \approx \theta_i$ for all i	Large		
Network adaptation	$z_i^* \approx$ constant, between θ^1 and θ^2 for all i	Small	Small	
Habitat specialization	$z_i^* \approx \theta^1$ or θ^2 for all i	Small	Large	Small
Mosaic specialization	$z_i^* \approx \theta^1$ or θ^2 for each i at the subnetwork level	Small	Large	Large

Note: We have here eliminated one of the parameters γ, σ_G^2, and δ by defining the scaled mean phenotype $\tilde{z}_i = z_i/\delta$ and the optimal phenotype as $\theta_i = \delta H_i$, where H_i has the values of 0 or 1. The parameter combinations are $\Gamma = \gamma\sigma_G^2$ and $\Delta = \gamma\delta^2/2$.

ferences in patch qualities (large δ in fig. 6). With low migration rate and hence little gene flow (fig. 6, *upper left corner*), populations become locally adapted. Keeping everything else the same but increasing migration rate leads to habitat specialization as a result of the high cost of maladaptation (fig. 6). In this case, migrant individuals that arrive at the wrong habitat type are poorly adapted and reduce population growth rate and lifetime, essentially leading to a source-sink metapopulation structure and to a network-level process of migrational meltdown described for a two-population model by Ronce and Kirkpatrick (2001). If the two habitat types are roughly equally common in the network, the asymmetry may evolve in both directions, and hence, the dynamics exhibit alternative stable states (fig. 6*C*). Finally, when migration rate and hence gene flow are very high, the metapopulation evolves network-level adaptation, with all populations having roughly the same value of z_i^*. With increasing migration rate and hence increasing colonization rate, the incidences of patch occupancy increase (fig. 6*D*).

If the correspondence between the phenotype of the immigrant and the optimal phenotype in the target patch influences colonization ($\beta > 0$; immigrant selection), the effect of gene flow in opposing local selection is reduced, as the contribution of poorly adapted individuals to gene flow and founder events is reduced (fig. 5, *third row*). In the case of previously unoccupied patches, immigrant selection reduces the overall colonization rate, but the new populations that become established are on average better adapted to the local conditions than would be the case with phenotype-independent colonization.

Effect of Landscape Structure

The default landscape structure involves three kinds of heterogeneity: variation in patch areas, random spatial locations of the patches, and random placement of the two kinds of habitat patches in the network. We examined how the model-predicted dynamics in figure 5 are affected by elimination of the different types of heterogeneity.

Removing the randomness in the spatial locations of the patches by assuming a regular grid changes the predicted dynamics very little (results not shown). Assuming that all patches have the same size but random spatial

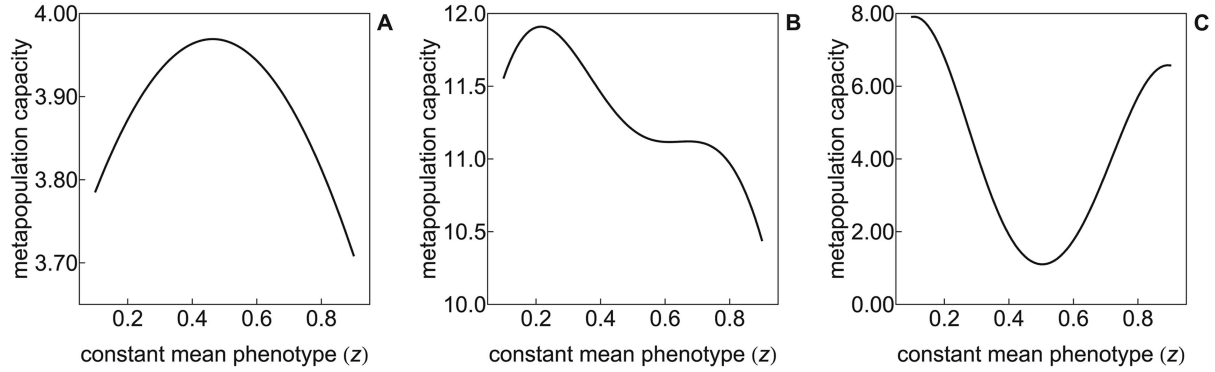

Figure 3: Metapopulation capacity of a patch network for metapopulations with the same constant mean phenotype (z) in all local populations. *A*, Low cost of maladaptation ($\gamma\delta^2 = 0.005, c = 0.0007$); *B*, intermediate cost of maladaptation ($\gamma\delta^2 = 0.05, c = 0.002$); *C*, high cost of maladaptation ($\gamma\delta^2 = 0.25$, $c = 0.002$). Note that in the first case, a species with intermediate z experiences the largest network as measured by the metapopulation capacity, while in the third case, the two specialists experience a larger network than the generalist. The patch network has the default structure and parameter values (table 1; $\alpha = 0.2$). The metapopulation capacity was calculated using the approximation presented in the text.

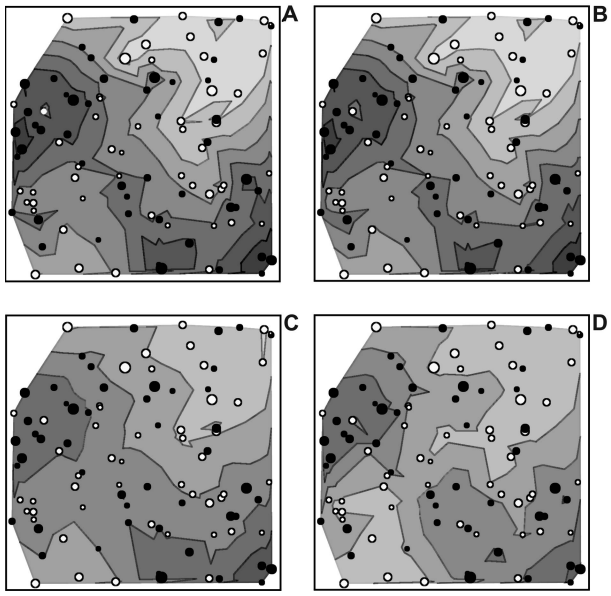

Figure 4: Example of model-predicted adaptation with short-range migration ($\alpha = 2$). The background color gives the spatially smoothened value of the mean phenotype (z_i^*), while the color of the patches indicates the optimal phenotype (θ_i). The result was calculated with (*A*) the deterministic approximation without gene flow ($\rho = 0$), (*B*) the corresponding stochastic model, (*C*) the deterministic approximation with gene flow ($\rho = 3$), and (*D*) the individual-based model described in appendix A in the online edition of the *American Naturalist*, which includes gene flow mechanistically. Parameter values in *A*–*C* are $\sigma_G^2 = 0.005$, $\gamma = 1$, and $c = 0.001$. Parameters of the individual-based model and their values are given in appendix A. The patch network has the default structure and parameter values (table 1).

locations somewhat increases the domain of habitat specialization and decreases the domain of mosaic specialization. Removing both kinds of heterogeneity reduces the parameter combinations that yield mosaic specialization into a small part of the parameter space with intermediate genetic variance. Finally, the most radical effect was obtained, as expected, by removing all heterogeneity. This was done by assuming a regular grid of equally large patches, with the two patch types placed in a regular chessboard fashion on the grid, and wrapping around the edges of the grid. In this case, there is no mosaic specialization, but habitat specialization occurs for small α, small σ_G^2, and large γ.

Metapopulation dynamics have to satisfy a threshold condition for long-term persistence (Hanski and Ovaskainen 2000), meaning that the colonization rate has to exceed the extinction rate when the size of the metapopulation is small. Habitat loss and fragmentation increase the extinction rate and decrease the colonization rate and hence pose a threat to metapopulation viability. In this context, we may ask about the consequences of the combined extinction-colonization dynamics and the dynamics of local adaptation for metapopulation persistence.

We constructed a range of increasingly unfavorable landscapes by increasing the size of the square area within which a particular network of 100 patches is located while keeping the scale of colonization constant ($\alpha = 1$). Thus, with increasing landscape size, the patches become increasingly isolated from each other. With increasing fragmentation, the incidences of patch occupancy decrease due to decreasing colonization rates (fig. 7). We compared the model predictions for two scenarios, with and without adaptive evolution. In the scenario without evolution, the mean phenotypic values were fixed at the patch-specific values predicted by the model for the most favorable landscape (though in the example shown in fig. 7, there is actually very little variation in the z_i^* values in the most favorable landscape). In the scenario with evolution, the mean phenotypic values were recalculated for each increasingly fragmented landscape.

The question is whether model predictions are different for the two scenarios. Figure 7 gives a representative example in which the species exhibits network adaptation in the most favorable landscape due to high rate of colonization and gene flow (fig. 7, *upper right-hand corner*). With increasing fragmentation and hence decreasing between-patch movements, the evolutionary dynamics lead to habitat specialization. In this region, the average incidences decline faster than in the scenario without evolution because while the species specializes into one habitat type, the patches representing the alternative type are little used. Thus, in this region, evolution reduces metapopulation viability. However, with further fragmentation, movements become ever more localized, and the type of adaptation changes to mosaic specialization, whereby the species specializes to use the more frequent habitat type at the subnetwork level. This leads to higher average incidences than without evolution (fig. 7), and thus, here evolution enhances metapopulation viability. Figure 7*B* shows the result for the corresponding stochastic model, in which metapopulations with very low incidences become extinct.

Comparisons between the Different Models

The above analyses are based on the deterministic approximation (derived in app. B) of the stochastic model (described in "Models"). How good is this approximation? We have compared the approximation with the stochastic model at length in appendix C. The two models become increasingly similar, as expected, when the scale of migration increases (fig. C1), and in general the approximation predicts patterns of adaptation very similar to those predicted by the stochastic model. The exceptions are multiple

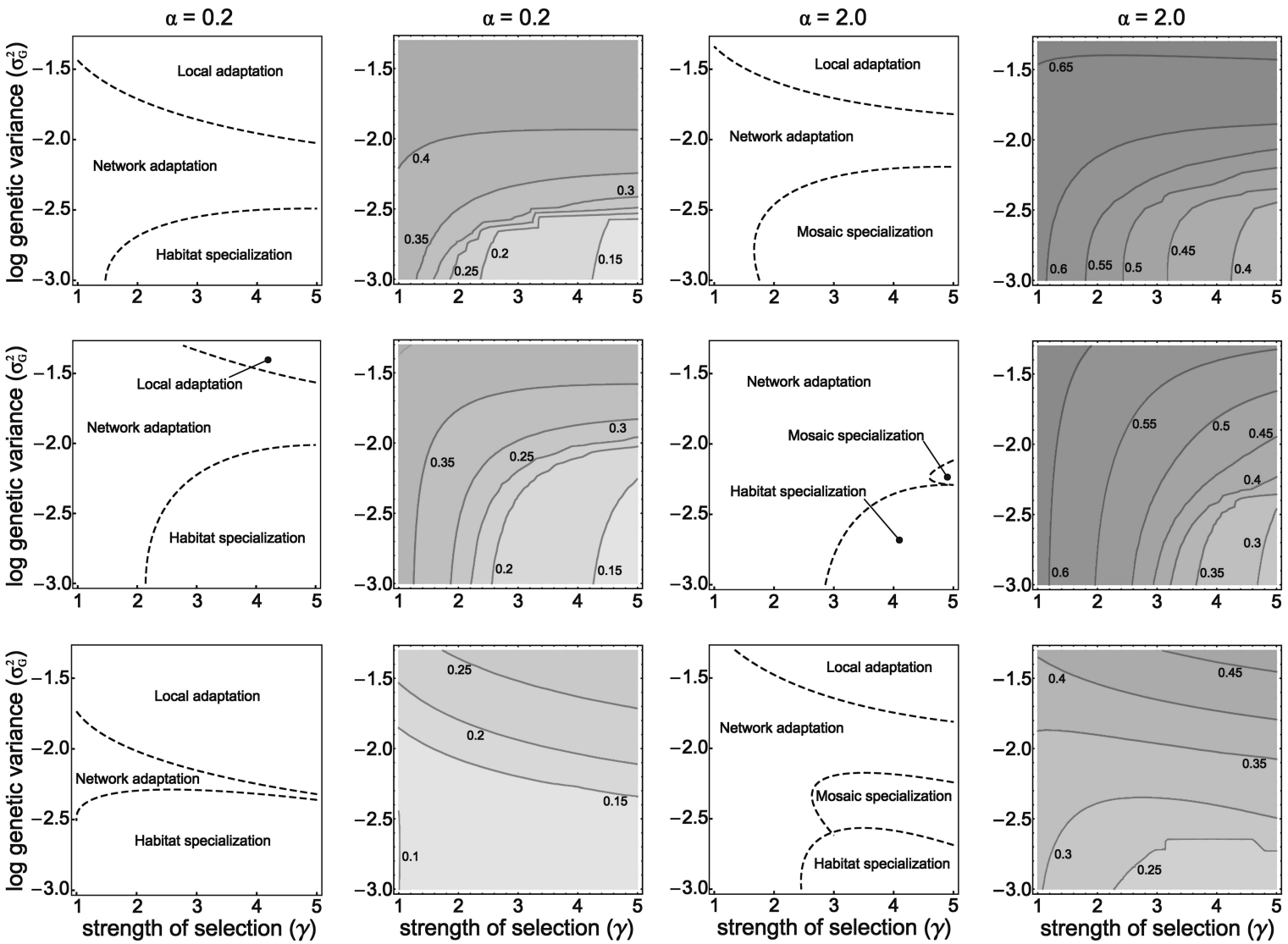
α = 0.2
α = 0.2
α = 2.0
α = 2.0
log genetic variance (σ_G^2)
strength of selection (γ)
Local adaptation
Network adaptation
Habitat specialization
Mosaic specialization
0.65
0.6
0.55
0.5
0.45
0.4
0.35
0.3
0.25
0.2
0.15
0.1

stable alternative equilibria predicted by the approximation for mosaic specialization, of which many equilibria have such small domains of attraction that the stochastic model does not spend much time within them (app. C). Nonetheless, even in this case, the stationary state of the stochastic model is very similar to the dominant stable equilibrium predicted by the approximation (cf. fig. 4*A*, 4*B*).

Another important question concerns the influence of constant genetic variance, a key assumption of both the stochastic model and its deterministic approximation. To address this question, we constructed an individual-based model (app. A) that assumes sexual reproduction and includes genetic drift, as well as an explicit description of local dynamics, including the individual-level consequences of migration and gene flow on demography and local adaptation. In this model, genetic variance is not constant but changes in time and space, depending on the sizes and composition of local populations. For instance, in the example in figure 4*D*, within-population genetic variance increases highly significantly with increasing patch area and connectivity, which together explain 66% of variation in genetic variance among the populations (see fig. A1). Nonetheless, the deterministic approximation with constant genetic variance predicts patterns of adaptation very similar to those predicted by the individual-based model. Figure 4*C*, 4*D* gives an example, further analyzed in appendix A. We conclude that the deterministic approximation performs well in predicting the qualitative patterns of local adaptation in spite of the simplifying assumptions of constant genetic variance and no genetic drift.

Discussion

We have constructed and analyzed a class of metapopulation models that combines classic extinction-colonization dynamics with the dynamics of adaptation to the environmental conditions prevailing in local habitat patches. Our model can be viewed as an extension of the model of two coupled populations by Ronce and Kirkpatrick (2001) to a network of many populations, though there is the difference that their deterministic model does not allow for local extinctions and our model does not include an explicit description of demographic dynamics in local populations. In both models, maladaptation decreases population growth rate, which in our model translates to an increased probability of local extinction. For simplicity, we model changes in the mean phenotype of local populations, but qualitatively similar results were obtained with an individual-based model in which genetic variance is modeled mechanistically (app. A).

The present model addresses a shortcoming of classic metapopulation models, which assume a network of habitat patches of the same quality. Many ecologists have called for models with spatial variation in habitat quality among the patches (Dennis and Eales 1999; Thomas et al. 2001; Fleishman et al. 2002). On the other hand, previous models of the evolution of ecological traits in patchy landscapes have assumed an idealized landscape structure, usually consisting of just two dissimilar patches (Holt and Gaines 1992; Kawecki 1995; Holt 1996; Ronce and Kirkpatrick 2001). The present model can be applied to patch networks of any size and any spatial configuration, allowing the study of, for example, the influence of the spatial scale of colonization and gene flow and the consequences of habitat loss and fragmentation on the eco-evolutionary dynamics.

Our main conclusion is that extinction-colonization dynamics in a heterogeneous patch network may interact with local selection to generate four different patterns of adaptation. In two cases, which we call "network adaptation" and "habitat specialization," the metapopulation is essentially monomorphic, the mean phenotype being either a generalist, representing a compromise between the two optimal phenotypes (network adaptation), or a specialist on one of the habitat types (habitat specialization). In both cases, the product $\gamma\sigma_G^2 T$ is relatively small, hampering strictly local adaptation. The demographic cost of maladaptation determines the type of adaptation, with low cost of maladaptation leading to network adaptation of a generalist species and high cost of maladaptation leading to habitat specialization. To distinguish between these two cases in empirical studies requires knowledge of spatial variation in habitat quality. For instance, working on female oviposition host plant preference in the Glanville fritillary butterfly, Hanski and Heino (2003) compared preference in 24 independent habitat patch networks with dissimilar relative abundances of the two host plant species. In the case of habitat specialization, preference for

Figure 5: Four patterns of adaptation (table 2) in relation to the strength of selection (γ), the amount of genetic variance (σ_G^2), and the range of migration ($1/\alpha$). The first two columns show the patterns of adaptation and the equilibrium incidences (p_i^*) for long-range migration ($\alpha = 0.2$); the last two columns show the respective results for short-range migration ($\alpha = 2$). The first row of panels gives the results without gene flow and immigrant selection, the second row with gene flow only ($\rho = 40$), and the last row with gene flow and immigrant selection ($\rho = 40, \beta = 3$). The delimitation of the different patterns of adaptation is based on the diagnostic variables described in appendix C in the online edition of the *American Naturalist*.

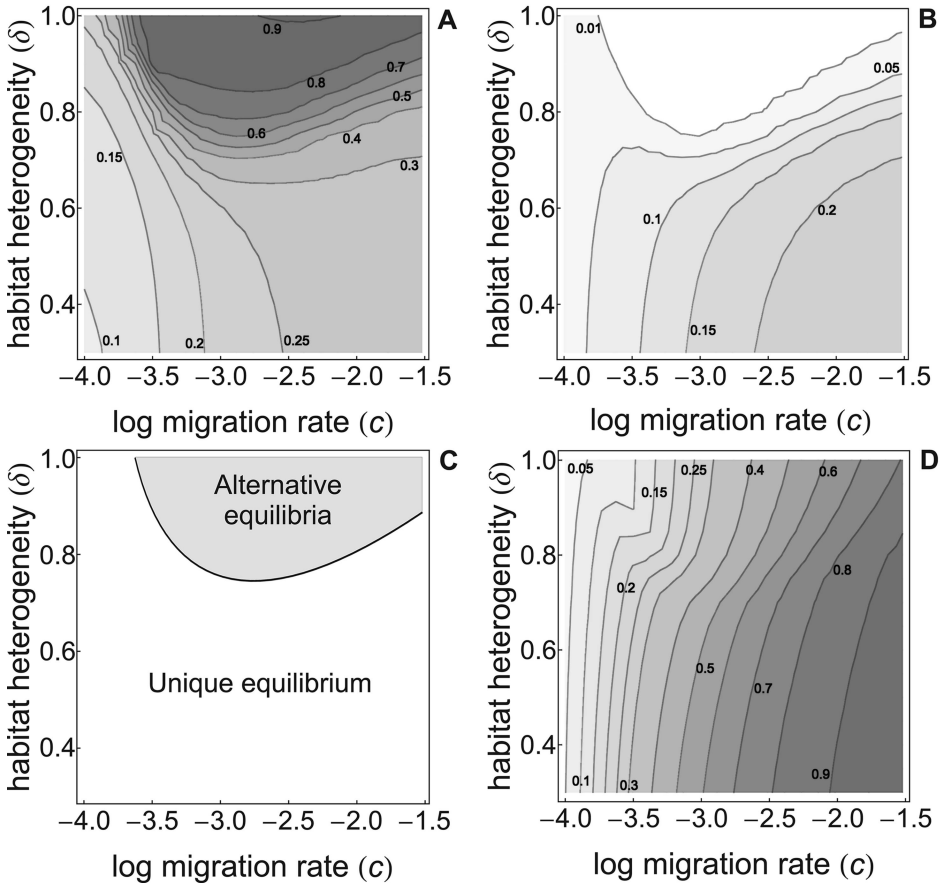

Figure 6: Effects of parameter c, which sets the migration and colonization rates, and habitat heterogeneity δ on the pattern of adaptation in the presence of gene flow in the deterministic model. *A*, *B*, Larger (S_L) and smaller (S_S) of the two sums $\sum_i (z_i^* - \theta_i)^2/\delta^2$ calculated separately for the two kinds of habitat patches. Note that in local adaptation both sums are small and in network adaptation both are moderately large, whereas in habitat specialization S_L is large and S_S is small (see table 2; app. C in the online edition of the *American Naturalist*). *C*, Parameter combinations that lead to alternative stable states (initial values: $z_i = \theta_i$ for all i and p_i small [large] for habitat type 1 [2] or vice versa). *D*, Equilibrium incidences (p_i^*). The other parameter values are $\gamma = 5$, $\alpha = 0.5$, $\sigma_G^2 = 0.01$, and $\rho = 50$. The patch network has the default structure and parameter values (table 1).

one host plant species switches abruptly to preference for the other species with changing relative abundances of the host plants in the networks (fig. 2*B*), whereas in network adaptation, the preference is proportional to the relative abundances (fig. 2*A*). The empirical and modeling results supported the latter (Hanski and Heino 2003, figs. 4, 5; see also Kuussaari et al. 2000). It is, however, important to note that the correspondence between habitat types and the mean phenotype in network adaptation is influenced by the spatial configuration of the network and exactly where in the network the different types of habitat patches are located, as this will affect the influence of particular populations on the dynamics of the metapopulation as a whole (Hanski and Heino 2003; Ovaskainen and Hanski 2003).

In the two other patterns of adaptation, the metapopulation is polymorphic, with either each local population being adapted to the respective habitat patch (when the product $\gamma\sigma_G^2 T$ is large) or the mean phenotypes in local populations being spatially correlated but largely independent of habitat quality. In the latter case, which we have dubbed "mosaic specialization" and which may arise when the spatial scale of colonization and gene flow is short, the species has become adapted to different habitat types in different parts of a large patch network, suggesting that the dynamics may have alternative stable states. Some of the empirical studies cited in the "Introduction" may exemplify mosaic specialization. Mosaic specialization is especially likely to occur in networks that have such highly aggregated spatial distribution of habitat patches that the

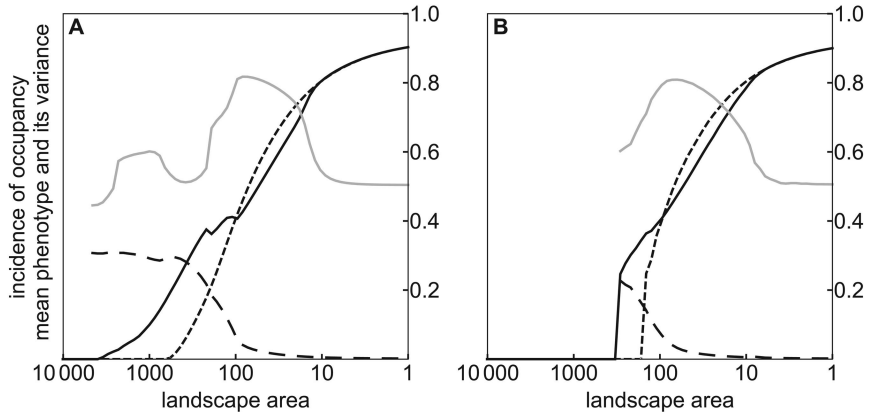

Figure 7: Metapopulation size as a function of the area of the landscape within which the default network of 100 patches is located (table 1). Thus, patch density in the network decreases to the left. *A*, *B*, Results for the deterministic approximation and the corresponding stochastic model. Metapopulation size is measured by the average incidence of patch occupancy weighted by patch areas. The small-dashed line gives the result for constant mean phenotypes, and the continuous line shows the model prediction in which the mean phenotypes are allowed to evolve. The gray and large-dashed lines give the average of the mean phenotype and its standard deviation across the network, respectively. The parameter values are $\alpha = 1$, $c = 0.001$, $\gamma = 5$, $\sigma_G^2 = 0.01$, $\rho = 80$, and $\beta = 0$.

patch aggregates harbor essentially independent metapopulations. However, our results demonstrate that no strongly aggregated patch distribution is required for mosaic specialization; random distribution is sufficient—in which case by just examining the physical structure of the network, it is not apparent which kind of spatially correlated pattern of adaptation might evolve at the network level.

Increasing gene flow is usually thought to make local adaptation less likely, as migrants bring poorly adapted genes to local populations (Räsänen and Hendry 2008; North et al. 2011). In the model of Ronce and Kirkpatrick (2001) for two populations, gene flow leads to migrational meltdown for a range of parameter values. Here, gene flow from the habitat patch with a larger and locally well-adapted population increases the frequency of maladapted individuals in the second population with different habitat quality, which decreases population size via the demographic cost of maladaptation, which further increases the frequency of poorly adapted migrant individuals, and so forth. Migrational meltdown with potentially alternative stable equilibria corresponds to the source-sink dynamics analyzed by Kawecki (1995), Holt (1996), Holt and Gomulkiewicz (1997), and others, in which gene flow prevents adaptation in the habitat with a small and poorly adapted population (sink population). For other parameter values, Ronce and Kirkpatrick's (2001) model exhibits a single equilibrium that is symmetric with respect to the two habitat types. Finally, for a range of limited gene flow between sufficiently dissimilar habitats, there are three alternative locally stable equilibria: the two asymmetric ones and the symmetric one.

Our model exhibits similar dynamics at the network level, though the two asymmetric alternative stable equilibria are not entirely identical because of heterogeneity in network structure. Clearly, limited habitat heterogeneity is not sufficient to eliminate the domains of alternative equilibria. Similarly, in the two-patch model of Ronce and Kirkpatrick (2001), asymmetric alternative equilibria were present even if there was some difference in the patch-carrying capacities. In both models, much gene flow leads to a generalist species using the two habitat types more or less equally (network adaptation).

The amount of gene flow between pairs of populations in a metapopulation is influenced by the intrinsic mobility of individuals, but similar population-level effects that are predicted by low mobility are also predicted by habitat fragmentation that decreases the density of patches in the network and hence limits the actual gene flow between populations. If we start with a landscape in which the metapopulation is adapted to use both habitat types because of much gene flow, reducing patch density may lead to habitat specialization, just as reducing the intrinsic rate of movements may have the same effect. Thus, a general prediction of the model is that habitat loss increases specialization. This has the demographic consequence of reduced metapopulation size across the network because the probabilities of occupancy are reduced in the patches to which populations are poorly adapted. In this scenario, evolutionary dynamics reduce metapopulation size. On the

other hand, when the patch network becomes very sparse, movements become increasingly restricted to the neighboring patches, which may lead to mosaic specialization that is, habitat specialization at the subnetwork level, which may boost metapopulation size in comparison with the scenario without adaptive evolution.

In summary, in the presence of strong coupling between the demographic dynamics and the genetic dynamics, adaptation to heterogeneous environmental conditions may occur at many spatial scales, from very local to the scale of the entire fragmented landscape. At which spatial scale adaptation is strongest depends on the amount of genetic variance, the strength of selection, the scale of gene flow, and the difference in the quality of dissimilar habitat patches. Regional adaptation that is not strongly related to the structure of the environment is reminiscent of Thompson's (2005) mosaic theory of coevolution, though it remains an open question how the present results would be altered by having two coevolving species with reciprocal interactions. The present models extend the incidence function model (Hanski 1994, 1999) and related ecological metapopulation models (Ovaskainen and Hanski 2004) to situations where the demographic dynamics are influenced by the evolutionary dynamics and vice versa (Saccheri and Hanski 2006; Pelletier et al. 2009). The ecological models have been fitted to empirical data on the incidences of patch occupancy (Etienne et al. 2004 and references therein). Similarly, the present eco-evolutionary models can, in principle, be fitted to empirical data on incidences of patch occupancy and degrees of local adaptation in heterogeneous patch networks.

Acknowledgments

We thank A. Hendry, A.-L. Laine, O. Ronce, J. Thompson, P. Thrall, and two anonymous reviewers for comments on the manuscript and the Academy of Finland (grants 131155, 38604, and 44887; Finnish Centre of Excellence Programmes 2000–2005, 2006–2011) and the European Research Council (AdG 232826 to I.H. and StG 205905 to O.O.) for funding.

Literature Cited

Bolnick, D. I., E. J. Caldera, and B. Matthews. 2008. Evidence for asymmetric migration load in a pair of ecologically divergent stickleback populations. Biological Journal of the Linnean Society 94: 273–287.

Byars, S. G., Y. Parsons, and A. A. Hoffmann. 2009. Effect of altitude on the genetic structure of an Alpine grass, *Poa hiemata*. Annals of Botany 103:885–899.

Dennis, R. L. H., and H. T. Eales. 1999. Probability of site occupancy in the large heath butterfly *Coenonympha tullia* determined from geographical and ecological data. Biological Conservation 87:295–301.

Diamond, J. M. 1984. "Normal" extinctions of isolated populations. Pages 191–246 *in* M. H. Nitecki, ed. Extinctions. University of Chicago Press, Chicago.

Edelaar, P., A. M. Siepielski, and J. Clobert. 2008. Matching habitat choice causes directed gene flow: a neglected dimension in evolution and ecology. Evolution 62:2462–2472.

Etienne, R. S., C. J. F. van ter Braak, and C. C. Vos. 2004. Application of stochastic patch occupancy models to real metapopulations. Pages 105–132 *in* I. Hanski and O. E. Gaggiotti, eds. Ecology, genetics, and evolution of metapopulations. Elsevier Academic, Amsterdam.

Fleishman, E., C. Ray, P. Sjögren-Gulve, C. L. Boggs, and D. D. Murphy. 2002. Assessing the roles of patch quality, area, and isolation in predicting metapopulation dynamics. Conservation Biology 16:706–716.

Foley, P. 1994. Predicting extinction times from environmental stochasticity and carrying capacity. Conservation Biology 8:124–137.

———. 1997. Extinction models for local populations. Pages 215–246 *in* I. Hanski and M. E. Gilpin, eds. Metapopulation biology. Academic Press, San Diego, CA.

Gandon, S., and Y. Michalakis. 2002. Local adaptation, evolutionary potential and host-parasite coevolution: interactions between migration, mutation, population size and generation time. Journal of Evolutionary Biology 15:451–462.

Gandon, S., Y. Capowiez, Y. Dubois, Y. Michalakis, and I. Olivieri. 1996. Local adaptation and gene-for-gene coevolution in a metapopulation model. Proceedings of the Royal Society B: Biological Sciences 263:1003–1009.

Gomulkiewicz, R., R. D. Holt, and M. Barfield. 1999. The effects of density dependence and immigration on local adaptation and niche evolution in a black-hole sink environment. Theoretical Population Biology 55:283–296.

Hanski, I. 1994. A practical model of metapopulation dynamics. Journal of Animal Ecology 63:151–162.

———. 1998. Connecting the parameters of local extinction and metapopulation dynamics. Oikos 83:390–396.

———. 1999. Metapopulation ecology. Oxford University Press, New York.

———. 2001. Spatially realistic theory of metapopulation ecology. Naturwissenschaften 88:372–381.

Hanski, I., and M. Heino. 2003. Metapopulation-level adaptation of insect host plant preference and extinction-colonization dynamics in heterogeneous landscapes. Theoretical Population Biology 64: 281–290.

Hanski, I., and O. Ovaskainen. 2000. The metapopulation capacity of a fragmented landscape. Nature 404:755–758.

———. 2003. Metapopulation theory for fragmented landscapes. Theoretical Population Biology 64:119–127.

Hanski, I., and M. Singer. 2001. Extinction-colonization dynamics and host-plant choice in butterfly metapopulations. American Naturalist 158:341–353.

Heino, M., and I. Hanski. 2001. Evolution of migration rate in a spatially realistic metapopulation model. American Naturalist 157: 495–511.

Hendry, A. P., T. Day, and E. B. Taylor. 2001. Population mixing and the adaptive divergence of quantitative traits in discrete populations: a theoretical framework for empirical tests. Evolution 55: 459–466.

Holt, R. D. 1996. Adaptive environments in source-sink environ-

ments: direct and indirect effects of density dependence on niche evolution. Oikos 75:182–192.

Holt, R. D., and M. S. Gaines. 1992. Analysis of adaptation in heterogeneous landscapes: implications for the evolution of fundamental niches. Evolutionary Ecology 6:433–447.

Holt, R. D., and R. Gomulkiewicz. 1997. How does immigration influence local adaptation? a reexamination of a familiar paradigm. American Naturalist 149:563–572.

Kawecki, T. J. 1995. Demography of source-sink populations and the evolution of ecological niches. Evolutionary Ecology 9:38–44.

Klemme, I., and I. Hanski. 2009. Heritability of and strong single gene (*Pgi*) effects on life-history traits in the Glanville fritillary butterfly. Journal of Evolutionary Biology 22:1944–1953.

Kuussaari, M., M. Singer, and I. Hanski. 2000. Local specialization and landscape-level influence on host use in an herbivorous insect. Ecology 81:2177–2187.

Laine, A. L. 2005. Spatial scale of local adaptation in a plant-pathogen metapopulation. Journal of Evolutionary Biology 18:930–938.

Lande, R. 1993. Risks of population extinction from demographic and environmental stochasticity and random catastrophes. American Naturalist 142:911–927.

Lande, R., and S. Shannon. 1996. The role of genetic variation in adaptation and population persistence in a changing environment. Evolution 50:434–437.

Leimu, R., and M. Fischer. 2008. A meta-analysis of local adaptation in plants. PLoS One 3:e4010.

Moilanen, A. 2004. SPOMSIM: software for stochastic patch occupancy models of metapopulation dynamics. Ecological Modelling 179:533–550.

Morgan, A. D., S. Gandon, and A. Buckling. 2005. The effect of migration on local adaptation in a coevolving host-parasite system. Nature 437:253–256.

Nieminen, M., M. Siljander, and I. Hanski. 2004. Structure and dynamics of *Melitaea cinxia* metapopulations. Pages 63–91 *in* P. R. Ehrlich and I. Hanski, eds. On the wings of checkerspots: a model system for population biology. Oxford University Press, New York.

North, A., J. Pennanen, O. Ovaskainen, and A. L. Laine. 2011. Local adaptation in a changing world: the roles of gene flow, mutation, and sexual reproduction. Evolution, doi:10.1111/j.1558-5646.2010.01107.x.

Nosil, P. 2009. Adaptive population divergence in cryptic color pattern following a reduction in gene flow. Evolution 63:1902–1912.

Ovaskainen, O., and I. Hanski. 2002. Transient dynamics in metapopulation response to perturbation. Theoretical Population Biology 61:285–295.

———. 2003. How much does an individual habitat fragment contribute to metapopulation dynamics and persistence? Theoretical Population Biology 64:481–495.

———. 2004. Metapopulation dynamics in highly fragmented landscapes. Pages 73–104 *in* I. Hanski and O. E. Gaggiotti, eds. Ecology, genetics, and evolution in metapopulations. Elsevier Academic, Amsterdam.

Ovaskainen, O., and B. Meerson. 2010. Stochastic models of population extinction. Trends in Ecology & Evolution 25:643–652.

Pelletier, F., D. Garant, and A. P. Hendry. 2009. Eco-evolutionary dynamics: introduction. Philosophical Transactions of the Royal Society B: Biological Sciences 364:1483–1489.

Räsänen, K., and A. P. Hendry. 2008. Disentangling interactions between adaptive divergence and gene flow when ecology drives diversification. Ecology Letters 11:624–636.

Riechert, S. E. 1993. Investigation of potential gene flow limitation of behavioral adaptation in an aridland spider. Behavioral Ecology and Sociobiology 32:355–363.

Ronce, O., and M. Kirkpatrick. 2001. When sources become sinks: migrational meltdown in heterogeneous habitats. Evolution 55:1520–1531.

Saccheri, I., and I. Hanski. 2006. Natural selection and population dynamics. Trends in Ecology & Evolution 21:341–347.

Schoener, T. E., and D. A. Spiller. 1987. High population persistence in a system with high turnover. Nature 330:474–477.

Singer, M. C., and I. Hanski. 2004. Dispersal behavior and evolutionary metapopulation dynamics. Pages 181–198 *in* P. R. Ehrlich and I. Hanski, eds. On the wings of checkerspots: a model system for population biology. Oxford University Press, New York.

Slatkin, M. 1977. Gene flow and genetic drift in a species subject to frequent local extinctions. Theoretical Population Biology 12:253–262.

Thomas, J. A., N. A. D. Bourn, R. T. Clarke, K. E. Stewart, D. J. Simcox, G. S. Pearman, R. Curtis, and B. Goodger. 2001. The quality and isolation of habitat patches both determine where butterflies persist in fragmented landscapes. Proceedings of the Royal Society B: Biological Sciences 268:1791–1796.

Thompson, J. N. 2005. The geographic mosaic of coevolution. University of Chicago Press, Chicago.

Thompson, J. N., S. L. Nuismer, and R. Gomulkiewicz. 2002. Coevolution and maladaptation. Integrative and Comparative Biology 42:381–387.

Thrall, P. H., J. J. Burdon, and J. D. Bever. 2002. Local adaptation in the *Linum marginale–Melampsora lini* host-pathogen interaction. Evolution 56:1340–1351.

Toju, H. 2008. Fine-scale local adaptation of weevil mouthpart length and camellia pericarp thickness: altitudinal gradient of a putative arms race. Evolution 62:1086–1102.

Tufto, J. 2000. Quantitative genetic models for the balance between migration and stabilizing selection. Genetical Research 76:285–293.

Yeaman, S., and F. Guillaume. 2009. Predicting adaptation under migration load: the role of genetic skew. Evolution 63:2926–2938.

Associate Editor: Yannis Michalakis
Editor: Ruth G. Shaw